NEW YORK UNIVERSITY
"N.Y. Geophysical Sciences Lab.
6379002
College of Engineering
RESEARCH DIVISION
University Heights, New York 53, N. Y.

61 p.

Department of Meteorology and Oceanography
Geophysical Sciences Laboratory, Report No. 63-10

; Its 63-10) OTS: $6.60 ph, 2.03 mf
[Links series]

AN ANALYSIS OF BREAKING ATMOSPHERIC WAVES

By

Richard S. Greenfield

Final Report

(NASA under Grant No. NsG-168-61)

BREAKERS PROJECT

Project Director: James E. Miller July 1963 61 p 11 refs

July 1963

The research reported in this document has been sponsored by National Aeronautics and Space Administration.

NEW YORK UNIVERSITY
COLLEGE OF ENGINEERING
RESEARCH DIVISION

Department of Meteorology and Oceanography
Geophysical Sciences Laboratory Report No. 63-10

AN ANALYSIS OF BREAKING ATMOSPHERIC WAVES

By

Richard S. Greenfield

Final Report

under Grant No. NsG-168-61

BREAKERS PROJECT

Project Director: James E. Miller

July 1963

The research reported in this document has been sponsored in part by National Aeronautics and Space Administration.

Table of Contents

List of Figures

Abstract

2/950

The basic partial differential equations are derived for an atmospheric gravity wave at the internal interface of a two-layer, incompressible model. The model has a plane, sloping, non-rotating lower boundary. These equations are numerically integrated by the method of characteristics for various values of: (1) the initial acceleration of the wave-generating-mechanism and (2) lower boundary slope.

An analysis is made for the effects of the modelling parameters on the point at which the wave begins to break. Formulas for the point of initial breaking are obtained by perturbation analysis of the characteristic equation of the partial differential equations of the gravity wave. The results for the perturbation solution compare quite well with the results of the numerical integration. A simple attempt is made to evaluate the plausibility of the hypothetical connection between the breaking atmospheric wave and the squall line.

1. Introduction

In the status report issued for this project, Miller and Greenfield (1962), the basic problem and method of attack were outlined. This report will cover the details of the problem, method of solution and results.

A solitary wave is defined hydrodynamically as a single elevation of fluid which, if properly started, will travel for a considerable distance in a uniform channel. The amplitude of this wave does not have to be small compared with the fluid. Some discussion of such a wave in the context of classical hydrodynamics may be found in Lamb (1945). A wave of this type will, in general, not conserve its form. In fact, since it is a gravity wave, the maximum amplitude will overtake the lesser amplitude, leading part of the wave eventually, resulting in the breaking of the wave.

In special cases, as shown by Lamb, maintenance of a permanent solitary wave can be achieved if proper vertical accelerations are introduced in the fluid. Abdullah (1955) has discussed both the permanent and breaking solitary wave in the atmosphere.

The atmospheric solitary wave is a small scale phenomenon relative to the horizontal dimensions of the synoptic features (cyclones, anticyclones, etc.) which the meteorologist normally deals with. Thus, only the relatively recent establishment of some experimental small scale observing networks provided evidence of the phenomena which are apparently associated with the solitary wave. From analysis of

data obtained from such a network, Tepper (1950) postulated a mechanism for the formation of squall lines. A squall line is a line of thunderstorms of strong intensity accompanied by high wind gusts, pressure rises, temperature falls, and heavy showers. These squall lines are normally associated with cold fronts, forming in the warm air ahead of the front roughly parallel to it. Tepper showed that most of the features of a squall line, which passed through a micro-scale observing network, could be explained by a gravity wave propagating on an inversion ahead of the front. According to Tepper a "pressure jump" will form in the wave when the slope of the leading edge approaches the vertical. It is his hypothesis that this pressure jump is identified as a squall line.

Abdullah (1955), as pointed out earlier, discussed both the permanent and breaking atmospheric solitary wave. The theory of the breaking solitary wave is the same as that of the pressure jump line. The theory is such that the governing equations lend themselves to the method of characteristics. By means of this method, the differential equations may be integrated to give unique solutions.

As pointed out by Abdullah, the breaking solitary wave would lead to a release of mechanical energy through the turbulence which results from the breaking process. This energy will be added to the process of the mechanical lifting of the air in contact with the propagating wave. By this means sufficient lifting may occur to release any conditional instability which may exist in the air above the wave. It is Abdullah's hypothesis that such a mechanism is capable of producing locally severe weather. Thus, Abdullah's theoretical reasoning supports

Tepper's ideas concerning squall lines.

It should be noted that both Tepper and Abdullah considered the propagation of the solitary wave over a horizontal plane underlying surface. Abdullah (1961) proposed that the effect of a sloping, underlying surface on the wave be investigated. The major portion of this report deals with that investigation.

2. Derivation of the equations

Consider two incompressible, homogeneous fluids, one below the other on an inclined non-rotating plane. Let a Cartesian coordinate system be established such that the origin is at some point on the inclined lower boundary. It is assumed that there is no variation in the y direction. Thus, the model appears as shown in Figure 1.

The interface between the lower fluid of density ρ and the upper fluid of density ρ_o is initially at a height of h_o. The upper boundary of the two layer atmosphere is at H which is much greater than h_o. The height of the inclined lower boundary is η which is a linear function of x.

The governing equations for the lower fluid are the equation of continuity:

$$\frac{\partial u}{\partial x} + \frac{\partial w}{\partial z} = 0 \qquad (1)$$

and the equations of motion:

$$\frac{\partial u}{\partial t} + u\frac{\partial u}{\partial x} = -\frac{1}{\rho}\frac{\partial p}{\partial x} \qquad (2)$$

$$\frac{1}{\rho}\frac{\partial p}{\partial z} + g = 0 \qquad (3)$$

where u and w are the horizontal and vertical wind components respectively, t is time, p is pressure, and g is the gravitational

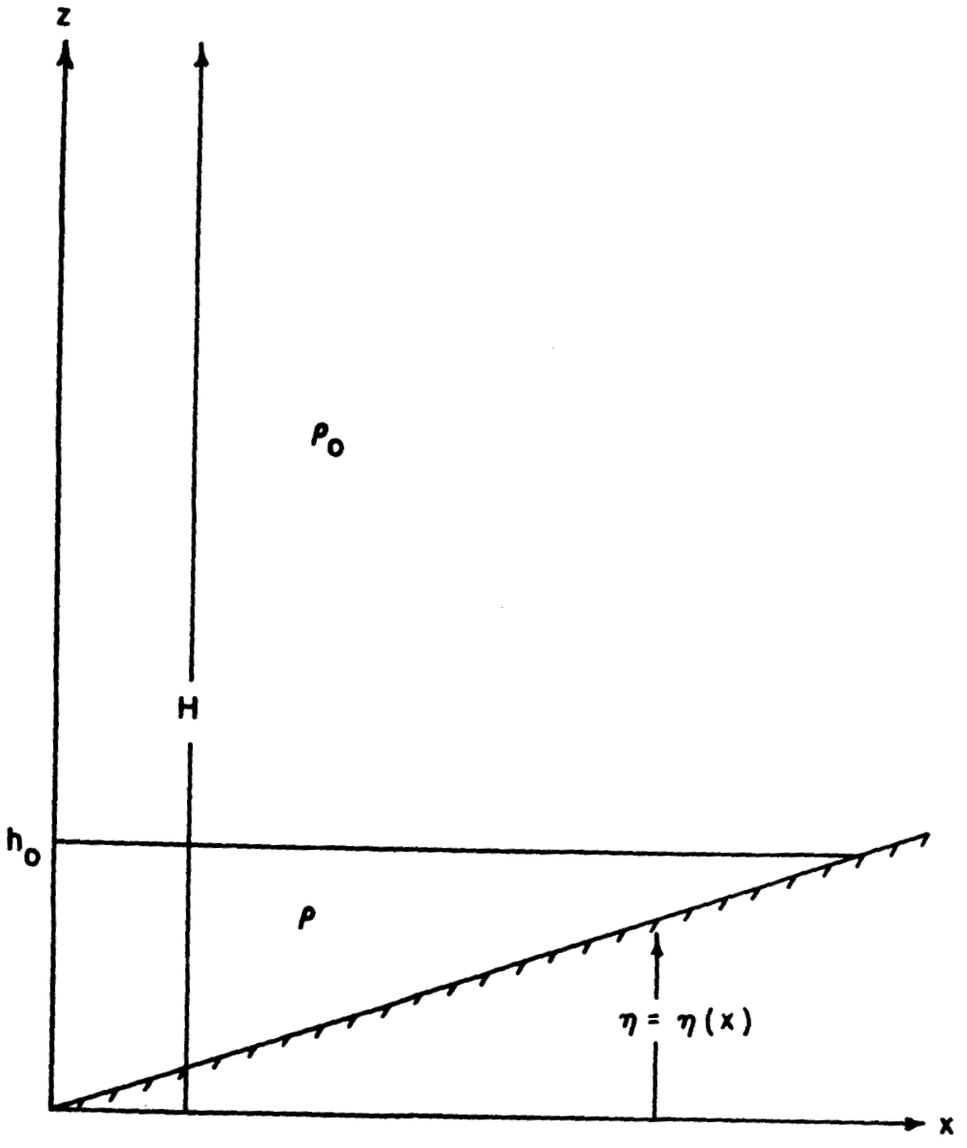

Figure 1. The model

acceleration.

Note that in equation (3) vertical accelerations have been neglected; i. e., the fluid is in hydrostatic equilibrium. As pointed out in the previous section, this assumption will not permit the permanent solitary wave.

Now, the equation of continuity, (1), is vertically integrated between the surface and the internal boundary, thus:

$$\int_{\eta}^{h} \frac{\partial u}{\partial x}\, dz + \int_{\eta}^{h} \frac{\partial w}{\partial z}\, dz = 0 \qquad (4)$$

where h is the height of the interface at any time. Consider the first term in (4). Applying Liebnitz' rule for differentiation of a definite integral (see Bronwell, 1953):

$$\int_{\eta}^{h} \frac{\partial u}{\partial x}\, dz = \frac{\partial}{\partial x} \int_{\eta}^{h} u\, dz - u \frac{\partial h}{\partial x} + u \frac{\partial \eta}{\partial x}$$

If we assume u is not a function of height (it shall be shown that this is true under the proper initial conditions), this last equation becomes:

$$\int_{\eta}^{h} \frac{\partial u}{\partial x}\, dz = \frac{\partial}{\partial x} [u (h - \eta)] - u \frac{\partial}{\partial x} (h - \eta) \qquad (5)$$

The second term in equation (4) becomes:

$$\int_{\eta}^{h} \frac{\partial w}{\partial z}\, dz = w_h - w_\eta$$

but

$$w_h \equiv \frac{dh}{dt} = \frac{\partial h}{\partial t} + u \frac{\partial h}{\partial x}$$

and

$$w_\eta \equiv \frac{d\eta}{dt} = u \frac{\partial \eta}{\partial x}$$

thus

$$\int_\eta^h \frac{\partial w}{\partial z}\, dz = \frac{\partial h}{\partial t} + u \frac{\partial}{\partial x} [h - \eta] \qquad (6)$$

Finally, substituting equations (5) and (6) in (4);

$$\frac{\partial h}{\partial t} + \frac{\partial}{\partial x} [u (h - \eta)] = 0 \qquad (7)$$

Now, if the hydrostatic equation (3) is integrated from the top of the model to some height z in the lower fluid.

$$\int_{p_z}^{p_H} dp = - \int_h^H \rho_o\, g\, dz - \int_z^h \rho\, g\, dz$$

Then,

$$p_H - p_z = - \rho_o\, g\, (H - h) - \rho\, g\, (h - z)$$

or

$$p_z = p_H + (\rho - \rho_o)\, g\, h + \rho_o\, g\, H - \rho g z \qquad (8)$$

Now if we assume H is at a height such that it is unaffected by horizontal variations in the lower fluid and that p_H is horizontally uniform, then from (8) it follows that:

$$\frac{\partial p}{\partial x} = (\rho - \rho_o)\, g\, \frac{\partial h}{\partial x}$$

Using this result in equation (2):

$$\frac{\partial u}{\partial t} + u\frac{\partial u}{\partial x} = - \frac{(\rho - \rho_o)}{\rho} g \frac{\partial h}{\partial x} \qquad (9)$$

From this equation, it is clear that if u is not initially a function of height it is never a function of height. This result was assumed a priori in the integration of the equation of continuity.

Defining a "density weighted" gravitational acceleration as:

$$g' \equiv \left(\frac{\rho - \rho_o}{\rho}\right) g$$

then equation (9) becomes:

$$\frac{\partial u}{\partial t} + u\frac{\partial u}{\partial x} + g'\frac{\partial h}{\partial x} = 0 \qquad (10)$$

The system of equations which describes the conditions within the lower fluid is made up of equations (7) and (10). According to Stoker (1948) this system of equations was first given, in a slightly different form, by Lagrange in 1781.

At this point the notation will be changed so that a subscripted variable will indicate partial differentiation with respect to that variable. The essentials of the following discussion and method of deriving the characteristic equations for the above system of equations can be found in Courant and Friedrichs (1948). It is of some interest to examine the basic concept involved in this method. Consider a function of two independent variables, x and t, say f(x,t). Now a linear combination, $a f_x + b f_t$, of the partial derivatives of f(x,t) means, geometrically, differentiation of f(x, t) in a direction given by the relationship $\frac{dx}{dt} = \frac{a}{b}$.

Analogously, if a curve is defined parametrically by $x(\sigma)$, $t(\sigma)$, with $dx:dt = a:b$ then $a f_x + b f_t$ is a derivative of f along this curve. In essence, the relationship between the coefficients of the partial derivatives is defined in such a way that the total derivative of the function is determined. Moreover, the total differentiation is along the defined curve.

Consider now the system of equations which has been derived above:

$$L_1 \equiv u_t + u u_x + g' h_x = 0 \qquad (10a)$$

$$L_2 \equiv h_t + [u (h - \eta)]_x = 0 \qquad (7a)$$

It is desired to determine a linear combination of this system of equations such that the derivatives of h and u, generally in two different directions, combine to derivatives in the same direction. This linear combination is given by:

$$L = \lambda_1 L_1 + \lambda_2 L_2$$

The direction which will be determined depends on the point x, t and the values of h and u at that point and is called a characteristic direction.

Forming the linear combination of the system of equations and grouping the coefficients by derivatives yields:

$$L = \lambda_1 u_t + [\lambda_1 u + \lambda_2 (h - \eta)] u_x + \lambda_2 h_t + [\lambda_1 g' + \lambda_2 u] h_x - \lambda_2 u \eta_x = 0$$

As discussed previously, it is desired to define characteristic curve $x(\sigma)$, $t(\sigma)$, such that:

$$\frac{dx}{dt} = \frac{\lambda_1 u + \lambda_2 (h - \eta)}{\lambda_1} = \frac{\lambda_1 g' + \lambda_2 u}{\lambda_2} \qquad (11)$$

Also since

$$d_\eta = \eta_x \, d_x$$

then

$$-\lambda_2 u = dx \qquad (12)$$

From (11) it follows that:

$$\lambda_1 dx - [\lambda_1 u + \lambda_2 (h - \eta)] \, dt = 0 \qquad (13)$$

and

$$\lambda_2 dx - (\lambda_1 g' + \lambda_2 u) \, dt = 0 \qquad (14)$$

Now rearranging equations (12), (13) and (14) in terms of λ_1 and λ_2:

$$(dx - u\,dt)\lambda_1 - [h - \eta)\,dt]\lambda_2 = 0 \qquad (15)$$

$$-g' \, dt \, \lambda_1 + (dx - u\,dt)\, \lambda_2 = 0 \qquad (16)$$

$$-u\lambda_2 = dx \qquad (17)$$

Since equations (15) and (16) are homogeneous, the determinant of the coefficients of these equations must vanish for λ_1 and λ_2 to exist or, i. e., for the direction $x(\sigma)$, $t(\sigma)$ to exist. Thus:

$$(dx - u\,dt)^2 - g' (h - \eta) \, dt^2 = 0$$

or

$$\left(\frac{dx}{dt}\right)^2 - 2u \frac{dx}{dt} + u^2 - g' (h - \eta) = 0$$

Solving for $\frac{dx}{dt}$:

$$\frac{dx}{dt} = u \pm \sqrt{g'(h - \eta)} \qquad (18)$$

This equation defines the family of characteristics in the x,tplane. Note that for the characteristics to be real, h must be greater than η. Physically, this is an obviously meaningful condition since it is clear that for a wave to exist on the internal boundary, this boundary must be above the underlying surface, i. e., h must be greater than η.

This particular condition also requires the original partial differential equations to be hyperbolic. Courant and Friedrichs have shown that a system of differential equations must be hyperbolic in order to apply the method of characteristics.

The family of characteristics which is defined by equation (18) is considered in terms of two sub-sets, namely the families of positive and negative characteristics. The positive family is defined by

$$C_+: \frac{dx}{dt} = u + c \qquad (19)$$

and the negative family by:

$$C_-: \frac{dx}{dt} = u - c \qquad (20)$$

where

$$c \equiv \sqrt{g'(h - \eta)} \qquad (21)$$

Equation (21) defines a propagation speed of a disturbance on the interface between the two fluids. It can readily be shown that if the equations for the model being used here had been derived in the manner of classical gas dynamics, the local "sound speed" would have been given by (21). Moreover, it can be shown that the differential

equations which have been derived, (7) and (10), are identical in form with the equations of gas dynamics for one-dimensional, compressible, adiabatic flow (Stoker, 1948). The physical meaning of equation (21) will be clarified shortly.

It is clear that to determine a positive or negative characteristic curve at any point (x,t) another equation is necessary for each sub-set since there are two dependent variables u and c (or h). While these "equations of compatability" can be derived by continuing in the manner of Courant and Friedrichs, doing so would involve a certain amount of tedious algebra. For the sake of brevity and additional physical interpretation, it is desirable to derive the equations of compatability as Stoker (1948) has done it.

It is now necessary to reformulate the system of differential equations (7a) and (10a) in terms of c. From equation (21):

$$c_x = \frac{1}{2c}(g'h_x - g'\eta_x) \tag{22}$$

and

$$c_t = \frac{g'h_t}{2c} \tag{23}$$

since η is independent of t.

If the quantities c, c_x, and c_t as defined by (21), (22) and (23) are introduced into (7a) and (10a) the following equations result:

$$u_t + uu_x + 2cc_x + g'\eta_x = 0 \tag{24}$$

$$2c_t + 2uc_x + cu_x = 0 \tag{25}$$

Now, if equations (24) and (25) are added the result can readily be put in the following form:

$$\left[\frac{\partial}{\partial t} + (u + c)\frac{\partial}{\partial x}\right](u + 2c + mt) = 0 \qquad (26)$$

Since η_x is constant in the model being considered, $g'\eta_x$ has been taken to be a constant, m.

Analogously, subtraction of (24) from (25) yields:

$$\left[\frac{\partial}{\partial t} + (u - c)\frac{\partial}{\partial x}\right](u - 2c + mt) = 0 \qquad (27)$$

Stoker (1948) shows that c represents the speed at which a disturbance propagates relative to the fluid whose speed is u.

The equations of compatability have now been derived. In summary, two families of characteristics, C_+ and C_-, have been derived on the x, t plane. They are defined by the following ordinary differential equations:

$$\left.\begin{aligned} C_+ &: \frac{dx}{dt} = u + c \\ C_- &: \frac{dx}{dt} = u - c \end{aligned}\right\} \qquad (28)$$

Moreover along these characteristics the following is true:

$$\left.\begin{aligned} u + 2c + mt &= k_1 = \text{const. along a given } C_+ \\ u - 2c + mt &= k_1 = \text{const. along a given } C_- \end{aligned}\right\} \qquad (29)$$

where $m \equiv g'\eta_x$. It is clear that the system (28) and (29) is exactly equivalent to the original system (7a) and (10a). Therefore, the solution of one system yields a solution of the other.

There are several important properties which make the use of the method of characteristics a particularly useful mathematical tool. These are:

1. As the finite differences used in approximating the

characteristic equations (28) and (29) approach zero, the solution for u and c of the finite difference scheme converge to the solution of the characteristic equations corresponding to the given initial or boundary conditions. It follows that for small enough finite differences solutions for u and c of the original system of equations can be determined by applying the method of characteristics. This property holds only if the prescribed initial boundary values of u and c are "sufficiently regular" functions of x and t. If these prescribed values are piecewise continuous they are sufficiently regular. (See Courant and Friedrichs, 1948).

2. The solutions of the finite difference approximations of the characteristic equation are always computationally stable, i. e., they will not grow indefinitely with time. This property has been explained by noting that the finite difference equations are such that the computational grid is being continuously modified by the equations in such a way that the space and time differences are always within the ratio prescribed by the computational stability criteria. The proof of the convergence of such solutions may be found in Sauer (1952), sec. 16.

As Courant and Friedrichs have shown, convergence of the characteristics indicates a compression wave, i. e., a disturbance resulting from compression of the fluid. Moreover, the point of

initial intersection of two characteristics, in the case of a model such as the one being used in this investigation, corresponds to the position and time of the onset of "breaking" of the atmospheric wave.

The importance of the breaking atmospheric wave was discussed in the introduction. For the purpose of this study, then, the position and time of breaking as obtained from the characteristic solution is of primary interest. This feature of the wave will be examined as it relates to variations in the model, particularly the slope of the underlying surface.

3. The wave generating mechanism

The mechanism which is employed to generate the disturbance on the interface is the same as that postulated by Abdullah (1955). The mechanism is a vertical density discontinuity which is an idealized model of a quasi-stationary front. It might be noted here that a vertical front cannot exist in the real atmosphere, but for the sake of simplicity such a front will be used in the model. This idealized front moves from the origin of the model into the initially stagnant two-layer atmosphere, thereby generating a compression wave on the internal interface.

After some time, the front stops and returns to its initial position producing, in the process, an expansion wave which follows the compression wave. Since this investigation is primarily concerned with the properties of the breaking wave, the expansion wave will not be considered.

The position of this front at any time is given by

$$x = a\left(1 - \cos \frac{c_o}{x_o} t\right) \tag{30}$$

where a is amplitude of the "frontal oscillation", x_o is some scale length, and c_o is some scale speed, both of which will be discussed in the next section.

It follows that the velocity of the front is:

$$\frac{dx}{dt} = \frac{c_o a}{x_o} \sin\left(\frac{c_o}{x_o}\right) \tag{31}$$

and the frontal acceleration is given by:

$$\frac{d^2x}{dt^2} = \frac{c_o^2 a}{x_o^2} \cos\left(\frac{c_o}{x_o} t\right) \tag{32}$$

4. The computational scheme

As discussed previously, the problem of determining the position and time at which the wave breaks becomes the problem of determining the point at which any two positive characteristics intersect. From the expression for the acceleration of the wave generating "front" (equation [32]), it is apparent that the maximum acceleration occurs initially (t = 0). The acceleration of the front then decreases with time. Under these conditions, it is reasonable to expect that breaking will first occur at the leading edge of the wave. Therefore, the position and time of initial breaking should be indicated by the intersection of the second and first positive characteristics.

It follows that the computational scheme should consist of numerically integrating the characteristic equations (28) and (29) in finite difference form to determine this intersection. The boundary condition is defined by the motion of the front (30). The numerical integration will be carried out until the intersection of the first and second positive characteristics is determined.

Before deriving the finite difference equations it is advantageous to make the continuous equations non-dimensional. Obviously, the solutions of the non-dimensional equations will be numerically more tractable and more importantly, they will be more generally applicable. In order to make the characteristic equations non-dimensional the following scaling parameters will be used:

1. $c_o \equiv \sqrt{g' h_o}$

where h_o = undisturbed height of the internal interface at the origin ($x = 0$), thus, c_o is the initial wave speed at the leading edge of the wave.

2. x_o, some arbitrary scale length.

Then making use of these parameters, the following non-dimensional variables are defined:

$$u^* \equiv u/c_o \qquad x^* \equiv x/x_o$$

$$c^* \equiv c/c_o \qquad t^* \equiv (c_o/x_o)t$$

$$g^* \equiv (x_o/c_o^2)\, g' = x_o/h_o$$

Substitution of these relationships into the characteristic equations (28, 29) results in the following non-dimensional characteristic equations for the two families of characteristics, C_+ and C_-:

$$\left.\begin{aligned} C_+ : \frac{dx^*}{dt^*} &= u^* + c^* \\ C_- : \frac{dx^*}{dt^*} &= u^* - c^* \end{aligned}\right\} \qquad (33)$$

and the non-dimensional equations of compatability:

$$\left.\begin{aligned} u^* + 2c^* + Gt^* &= k_1 \quad \text{along a given } C_+ \\ u^* - 2c^* + Gt^* &= k_2 \quad \text{along a given } C_- \end{aligned}\right\} \qquad (34)$$

where $G \equiv \dfrac{x_o \eta_x}{h_o}$

Now a non-dimensional amplitude for the "frontal oscillation" is defined as:

$$a^* \equiv a/x_o$$

Then substitution of this definition and the definition for the non-dimensional time, t^*, into the equation for the frontal motion (30) yields:

$$x^* = a^* (1 - \cos t^*) \qquad (35)$$

and along the boundary curve

$$u^* = a^* \sin t^* \qquad (36)$$

Then, the system of non-dimensional equations (33) and (34) is a closed set which can be solved by numerical integration.

Equations (35) and (36) represent analytic boundary conditions. It is necessary to specify an initial condition in order to solve the system. The initial condition which is used is that the fluids are at rest.

Under these conditions, the "initial characteristic", i. e., the positive characteristic in the x,t plane which separates the region of rest from the disturbed region, can be explicitly derived. This characteristic represents, physically, the leading edge of the wave. Along this characteristic, by the initial condition, $u^* = 0$. Therefore, from equation (33), the differential equation for this characteristic is:

$$\frac{dx^*}{dt^*} = c^* \tag{37}$$

and from equation (34) along the initial characteristic:

$$2c^* + Gt^* = k_1 \tag{38}$$

It is obvious that this characteristic must pass through the origin ($x^* = t^* = 0$) since the wave is generated from that point. Also at the origin $c^* = 1$ from the definitions of c^* and c_o. It follows, then, from equation (38) that $k_1 = 2$ and:

$$c^* = 1 - 1/2\ Gt^* \tag{39}$$

Then combining equations (37) and (39) yields:

$$\frac{dx^*}{dt^*} = 1 - 1/2\ Gt^*$$

which can be integrated yielding the equation for the initial characteristic:

$$x^* = t^* - \frac{Gt^{*2}}{4} \tag{40}$$

Therefore, the initial characteristic is a parabola whose vertex is at $x^* = 1/G = h_o/x_o\eta_x$.

It was pointed out in the derivation of the characteristic equations that in order to insure that the original system of equations be hyperbolic and to maintain a physically realistic model the underlying surface must not intersect the internal interface, i.e., $\eta = \eta_x x < h_o$ Therefore, x_L, the limiting value of x is given by:

$$x_L = \frac{h_o}{\eta_x}$$

If x_L is made non-dimensional:

$$x^*_L = \frac{h_o}{x_o\eta_x} \qquad (41)$$

Thus, it is clear that the vertex of the initial characteristic occurs at the point x^*_L which can be considered the horizontal limit of the model. This is physically realistic since this essentially means there can be no propagation of the disturbance beyond that point.

It is clear from equation (40) that the initial characteristic may be discretely generated by taking a finite time interval, say δt^*, and letting

$$t^* = N\,\delta t^* \qquad N = 0,\ 1,\ 2,\ ---$$

in equation (39). From this point on all variables will be non-dimensional and asterisks will be eliminated. Now the first point on the second characteristic must be determined. Consider the following diagram (Figure 2):

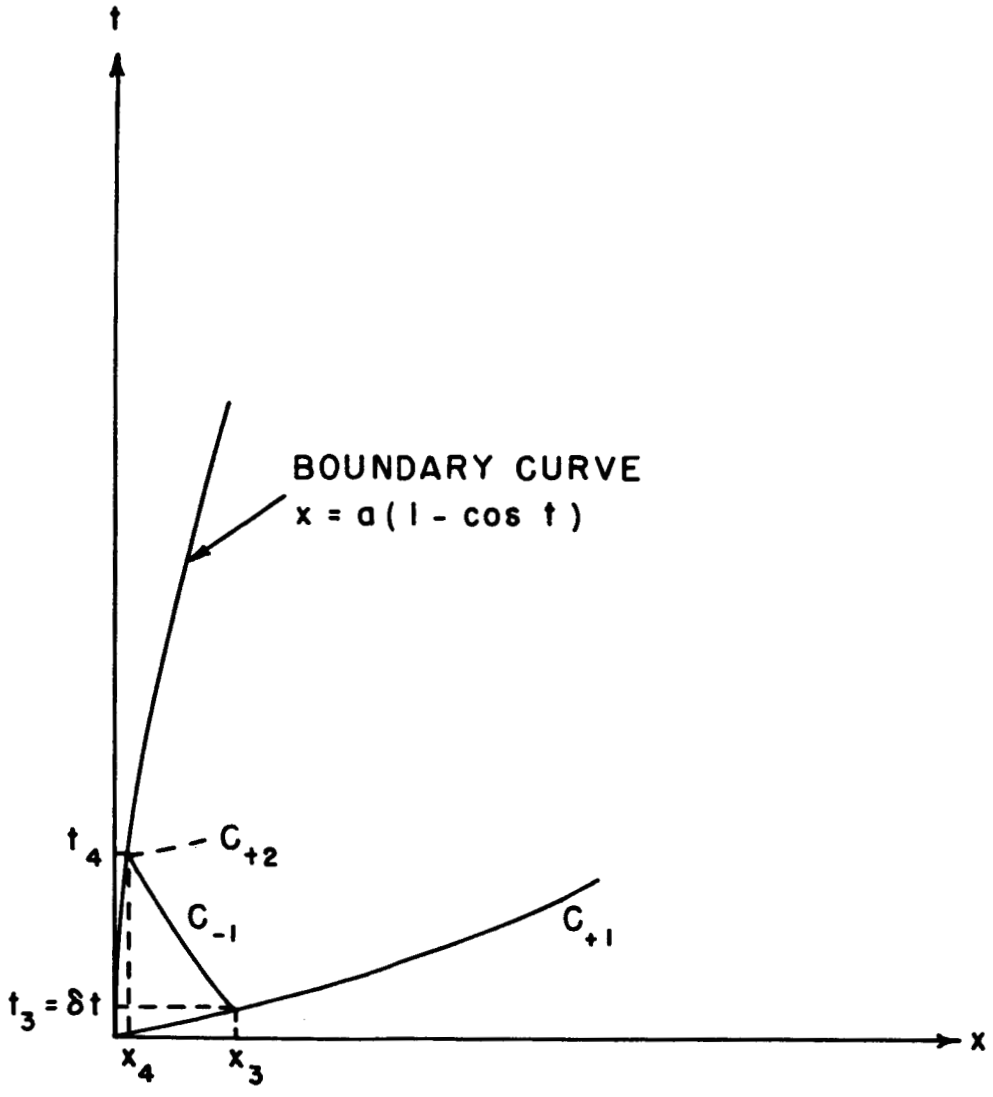

Figure 2. Determination of the foot of C_{+2}.

For the sake of clarity later, the point on the first characteristic will be designated by the subscript 3 and the first point on the second characteristic will be designated by the subscript 4. Note that the first point on the second characteristic (x_4, t_4) is determined by the intersection of the negative characteristic emanating from (x_3, t_3) and the boundary curve.

Prior to considering the system of equations which must be solved to determine the first point on the second characteristic, it is necessary to express the differential equations for the characteristics (33) in finite difference form. It will be assumed that the spatial and temporal scales are sufficiently small so that the generally curved characteristics can be approximated by straight line segments between the computational points. It will further be assumed that the slope of the straight line segment be approximated by the mean of the slopes at the end points. Consider the general situation as shown in Figure 3. In this diagram the values at point 4 are the unknowns thus, the pertinent positive characteristic line segment is between 2 and 4 and the pertinent negative characteristic line segment is between 3 and 4. Using these numbers as identifying subscripts and under the above mentioned assumptions equations (33) become (again ignoring the asterisks):

$$C_+ : (x_4 - x_{2)} = 1/2\,(u_4 + c_4 + u_2 + c_2)\,(t_4 - t_2) \qquad (42a)$$

$$C_- : (x_4 - x_3) = 1/2\,(u_4 - c_4 + u_3 - c_3)\,(t_4 - t_3) \qquad (42b)$$

Also, if the subscripts are applied to the equations of compatability (34) they become:

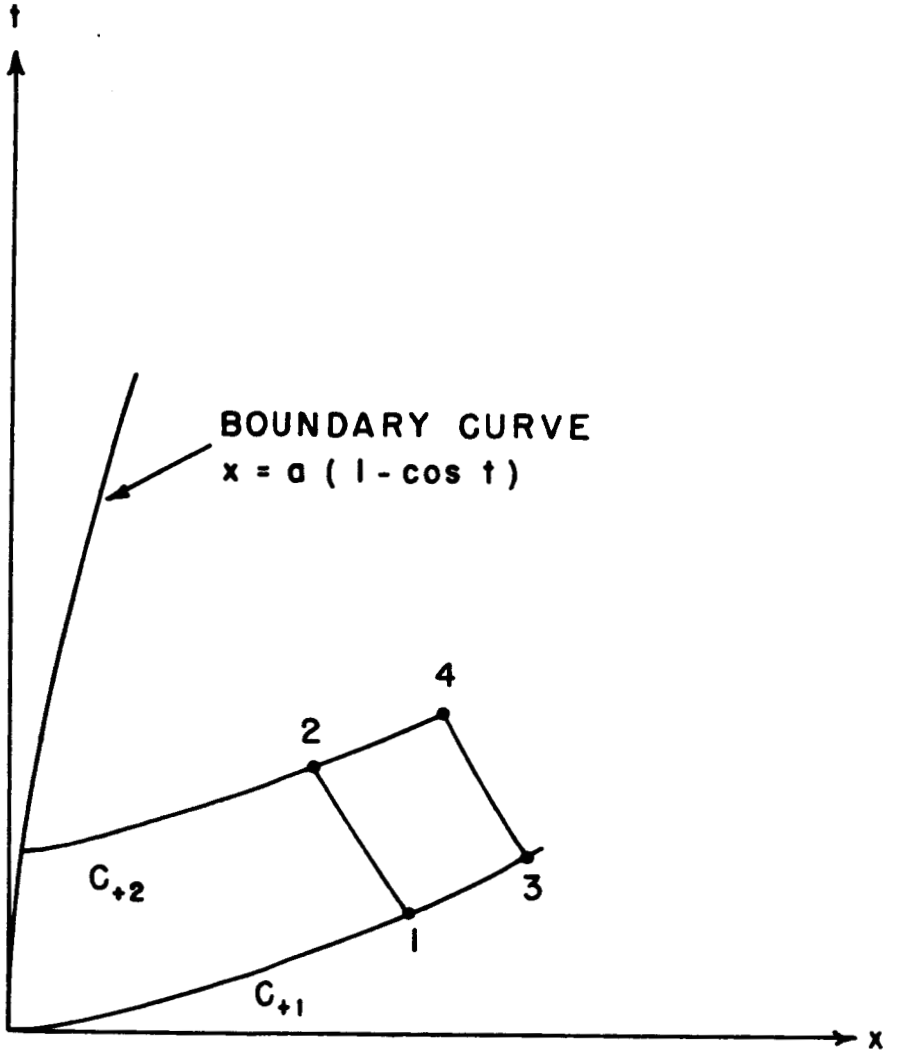

Figure 3. Schematic of general situation on characteristic plane.

$$u_4 + 2c_4 + Gt_4 = u_2 + 2c_2 + Gt_2 \text{ along } C_+ \tag{43a}$$

$$u_4 - 2c_4 + Gt_4 = u_3 - 2c_3 + Gt_3 \text{ along } C_- \tag{43b}$$

In the case where point 4 is on the boundary curve, the equations which apply along the boundary curve (35) and (36) become:

$$x_4 = a(1 - \cos t_4) \tag{44}$$

$$u_4 = a(\sin t_4) \tag{45}$$

The positive characteristic between 1 and 3, in the scheme being used here, is the initial characteristic. The generation of this characteristic has already been discussed. To complete the system of computation equations, the equations for generating the initial characteristic using the subscript notation follow from (39) and (40):

$$x_3 = t_3 - \frac{G}{4} t_3^2 \tag{46}$$

$$c_3 = 1 - \frac{G}{2} t_3 \tag{47}$$

and of course the generating mechanism is

$$t_3 = t_1 + \delta t \tag{48}$$

where δt is the specified time interval.

Returning now to the problem of determining the first point on the second characteristic, from the previous discussion the closed system of equations is made up of: (42b), (43b), (44) and (45). In this system from the initial condition $u_3 = 0$. The unknowns which must be determined are x_4, t_4, u_4, and c_4. Algebraic operations on the system leads to a single equation in one unknown, t_4:

$$2a[2\cos t_4 + 1/2(t_4 - t_3)\sin t_4] = 4a - 4x_3 + At_3 - [A + G(t_3 - t_4]t_4 \tag{49}$$

where $A = Gt_3 - 4c_3$.

This is a transcendental equation in t_4, with a trigonometric function

of t_4 on the left hand side and an algebraic function of t_4 on the right hand side. The solution for t_4 may be reasonably approximated from (49) by a straightforward iteration scheme. An initial guess for t_4 is made. Since it is known that $t_4 > t_3$ the first guess for t_4 is t_3. By an orderly series of steps the approximation is improved so that finally the error in t_4 is no more than $\pm$ 0.002.

Upon determining t_4 from (49), x_4 and u_4 follow directly from (44) and (45) respectively. Now knowing x_4, t_4 and u_4, from equation (43b) c_4 can be directly computed. The first point on the second characteristic has now been fully determined. Now those points which were subscripted 3 become subscripted 1 and those which were subscripted 4 become subscripted 2. Then by equations (46), (47) and (48) the next point on the first characteristic is generated and subscripted 3. Thus, the situation is as shown in Figure 3 with point 4 the unknown point. The closed system of equations which must be solved for x_4, t_4, u_4, c_4 are (42a and 42b) and (43a and 43b). To simplify the computation the right hand side of (43a) is determined just once as a constant from the values at the first point on the second characteristic. Thus immediately after determining that point the constant is computed so that equation (43a) is replaced by:

$$u_4 + 2c_4 + Gt_4 = Z \qquad (43a)$$

where Z is the constant. The algebraic operations involved in solving this system will not be displayed here. The resulting equations are shown in the program found in the appendix of this report. Starting from the changing of the subscripts, the entire operation of

determining x_4, t_4, u_4, and c_4 is to be found from statement number 43 through two statements before statement number 66.

The final part of the scheme, and in fact the part which will yield the results with which this report is concerned, involves the determination of the values at the intersection of the second and first characteristics.

The nature of the characteristics is such that, prior to intersection, t_4 must be greater than t_3 whereas after intersection the reverse is true. Thus, after the computation of the values at point 4 a test of the sign of $(t_3 - t_4)$ is used to determine whether intersection has already occurred. If $(t_3 - t_4)$ is negative the change of subscripts is effected and the next point is determined. If $(t_3 - t_4)$ is positive the intersection is determined. If $(t_3 - t_4)$ is zero x_4 and t_4 are printed out as the intersection values.

In the case where the values at intersection must be determined the following system of equations is solved:

$$xx - x_1 = (u_1 + c_1)\,(tt - t_1) \tag{50}$$

$$xx - x_1 = (u_2 + c_2)\,(tt - t_2) \tag{51}$$

These equations are the finite difference form of the differential equations for the positive characteristics emanating from points 1 and 2 (see Figure 3) and intersecting at the point xx, tt. Clearly, if x_4, t_4 has been determined to be beyond the intersection point, the points 1 and 2 must be used to determine the intersection. Also, since at intersection u and c are multi-valued, it must be assumed that the slopes of the two straight line approximations have

the values at the points 1 and 2 respectively. As the program was written, the final computation of the breaking point includes the transformation of the non-dimensional values, xx and tt, to dimensionalized values, xx_1 and tt_1. Equations (50) and (51) are readily solved for xx and tt. The resulting equations are shown in the program in the appendix.

This completes the description of the computational scheme. A more general scheme for solving for all the characteristics was originally developed, programmed and run on the Institute for Space Studies IBM 7090. Subsequently, an error was discovered in the basic equations. In the course of redeveloping the computational scheme it was decided to limit the investigation to the point of initial breaking. The FORTRAN program, which had originally been written, was modified to correct the error which was discovered. Also, the corrected program was revised for use on the IBM 1604 which was available at NYU's Heights Academic Computing Facility. This program is presented in the appendix. For additional understanding of the computational scheme and the program a flow diagram is presented in Figure 4.

5. The experiments and results

There were three series of experiments put through the model. Each series involved computing the initial breaking point for various underlying slopes. The distinguishing property between the three series was the amplitude of the "frontal oscillation" i. e., the maximum displacement of the wave generating mechanism. As can be seen from equations (31) and (32) this involves changing the

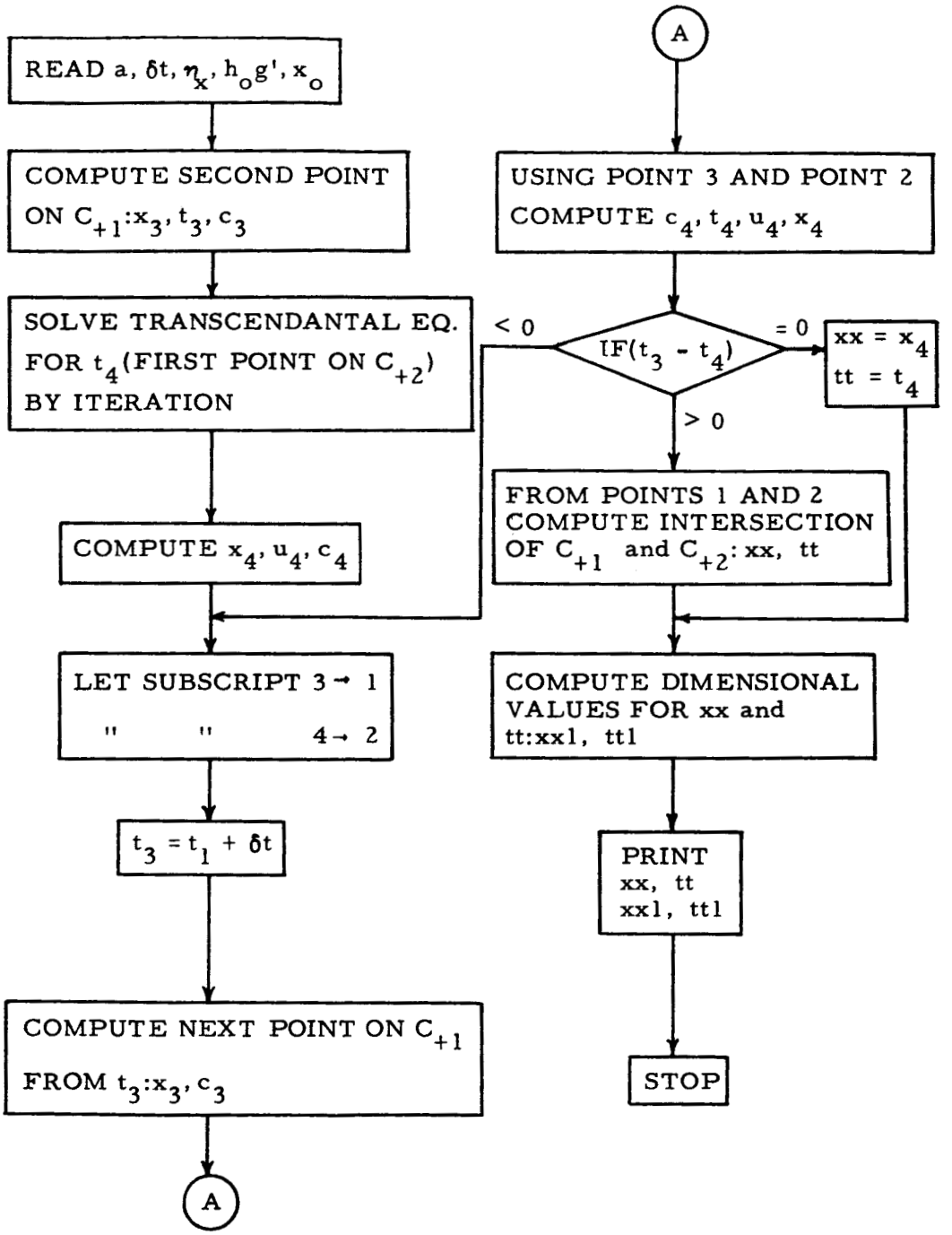

Fig. 4. Flow diagram of the computational scheme for determining initial point of breaking.

the velocity and acceleration of the "front".

In the first series, the amplitude, a, was taken to be 5 km, just as Abdullah (1955) originally used. The second and third series used 10 km and 20 km respectively. The scale length, x_o, was 10 km in all cases and h_o, the undisturbed height of the internal interface at the origin, was 2 km. The density difference across the internal interface, $(\rho - \rho_o)/\rho$, was taken to be 0.0156 just as Abdullah used. This corresponds to a temperature inversion of 4.1°C at the interface if the lower air mass has a mean temperature of 270°A. This figure does not enter the non-dimensional computations but it is used in converting the results to dimensionalized variables.

Various values for the time interval, δt^*, used to generate the first characteristic were tested. It was found that the changes in the breaker values were about 1 percent in going from a δt^* of 0.02 to a δt^* of 0.01 for the maximum and minimum values of the underlying slope. A δt^* of 0.002 led to changes in breaker values of about 0.6 percent from the values for a δt^* of 0.01. However, the amount of computer time to run each case increased to six minutes for a δt^* of 0.002 as compared to approximately one minute for a δt^* of 0.01. It was therefore decided to use a δt^* of 0.01 in all cases.

The last two series of experiments were done for one-half of the slope variations used in the first. The results of the computations are found in Table I. The non-dimensional results are presented graphically in Figures 5 and 6. In the graphs x_b^*

Table I: Computational Results

η_x	a = 5 km; $a^* = 0.5$				a = 10 km; $a^* = 1.0$				a = 20 km; $a^* = 2.0$			
	x_b^*	t_b^*	x_b km	t_b sec	x_b^*	t_b^*	x_b km	t_b sec	x_b^*	t_b^*	x_b km	t_b sec
0	1.35	1.35	13.5	770.0	0.68	0.68	6.8	388.8	0.346	0.346	3.46	198.1
.01	1.27	1.29	12.7	737.7								
.02	1.21	1.25	12.1	711.8	0.64	0.65	6.4	373.6	0.337	0.340	3.37	194.2
.03	1.15	1.20	11.5	686.1								
.04	1.09	1.16	10.9	662.4	0.61	0.63	6.1	359.6	0.328	0.333	3.28	190.6
.05	1.04	1.12	10.4	640.3								
.06	1.00	1.08	10.0	619.7	0.58	0.61	5.8	346.8	0.319	0.327	3.19	187.0
.07	0.95	1.05	9.5	600.5								
.08	0.92	1.02	9.2	582.6	0.55	0.59	5.5	334.9	0.311	0.321	3.11	183.6
.09	0.88	0.99	8.8	565.7								
.10	0.85	0.96	8.5	549.9	0.53	0.57	5.3	323.8	0.303	0.316	3.03	180.4
.11	0.82	0.94	8.2	535.0								
.12	0.79	0.91	7.9	520.9	0.50	0.55	5.0	313.5	0.296	0.310	2.96	177.3
.13	0.76	0.89	7.6	507.6								
.14	0.73	0.87	7.3	495.0	0.48	0.53	4.8	303.9	0.298	0.305	2.89	174.2
.15	0.71	0.85	7.1	483.0								
.16	0.69	0.82	6.9	471.7	0.46	0.52	4.6	294.9	0.282	0.300	2.82	171.4
.17	0.67	0.81	6.7	460.9								
.18	0.65	0.79	6.5	450.6	0.44	0.50	4.4	286.5	0.275	0.295	2.75	168.5
.19	0.63	0.77	6.3	440.7								
.20	0.61	0.75	6.1	431.4	0.43	0.49	4.3	278.6	0.269	0.290	2.69	165.8

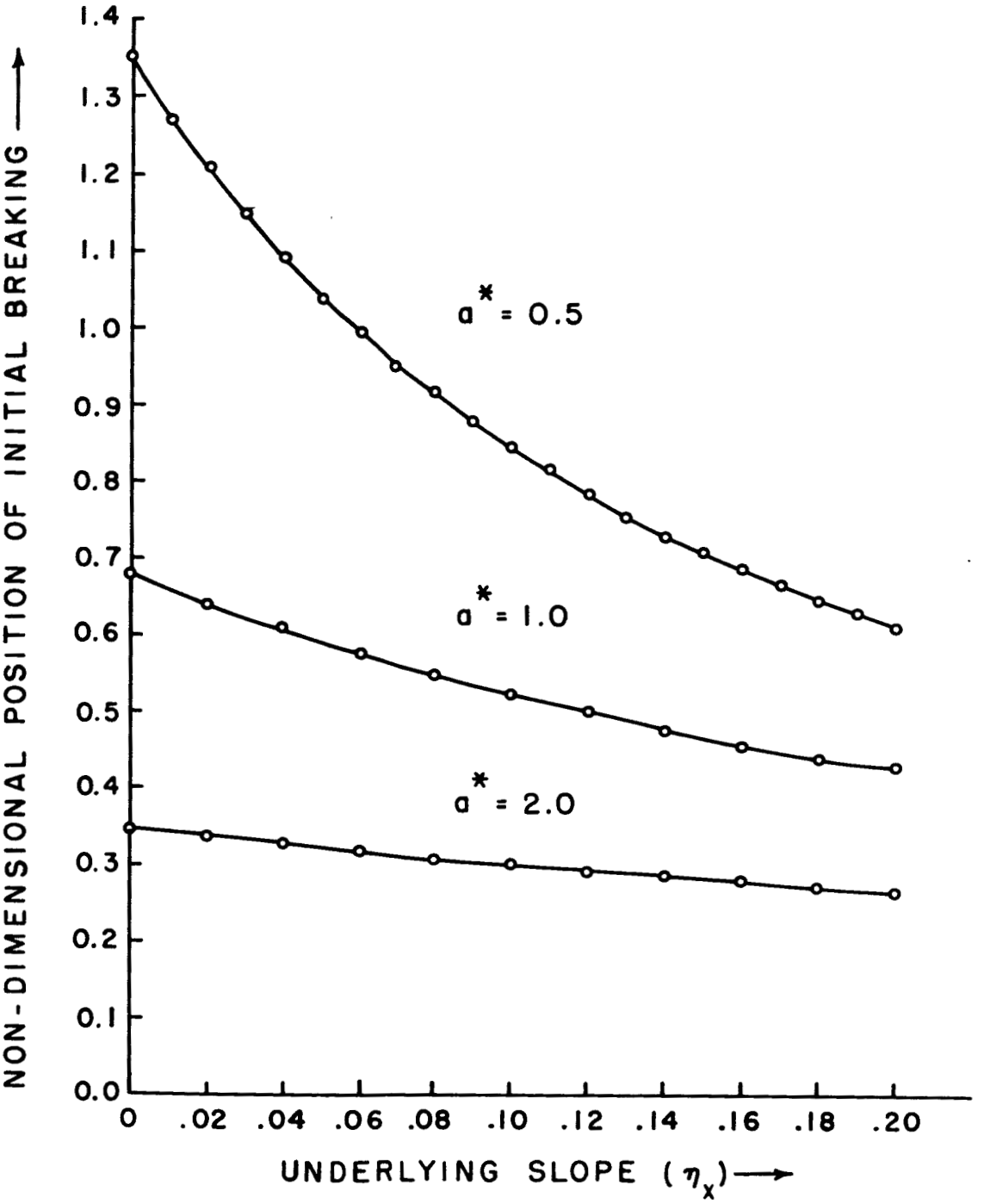

Figure 5. Non-dimensional initial breaking position as a function of underlying slope for various values of a* as obtained by numerical integration.

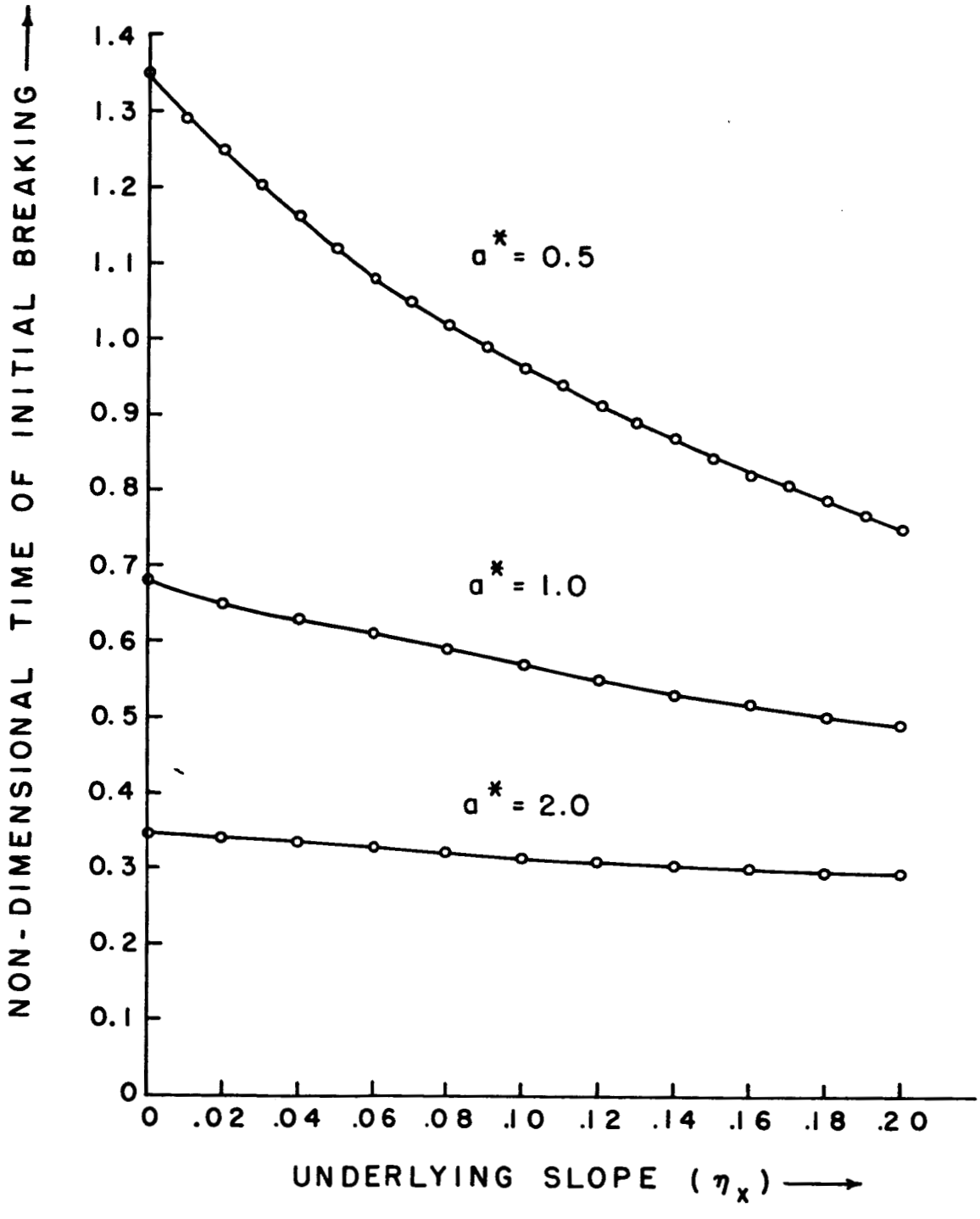

Figure 6. Non-dimensional initial breaking time as a function of underlying slope for various values of a* as obtained by numerical integration.

and t_b^* are plotted against the underlying slope. The subscript b refers to the breaking position.

The results were, in general, as anticipated. The time of breaking decreases as the slope increases. Since the position of breaking is dependent on the time of breaking, as the slope increases the disturbance breaks closer to the origin. Obviously, as the underlying slope approaches infinity, the time and position of breaking approaches the origin.

The non-linear effects of the underlying slope on breaking position and time are clearly seen in both figures. The decrease in breaking position and time as the slope increases is much larger for small slopes than for large slopes. Another feature which is clearly seen in the graphs is that the initial acceleration of the "front" bears a non-linear relation to the position and time of breaking. As the initial acceleration increases, the decrease in breaking position and time is diminished. Finally, the initial acceleration of the front is apparently a more dominant factor than the underlying slope in determining the position and time of initial breaking. However, as the acceleration decreases the underlying slope becomes increasingly important in determining x_b^* and t_b^*.

It was decided that an attempt would be made to derive an approximate solution for the point of initial breaking. If successful, this approximation might be useful for gaining a better understanding of the interaction between the initial frontal acceleration and the underlying slope as they affect the point of initial breaking. The derivation of the approximation appears in the next section.

6. A perturbation solution for the point of initial breaking

In this derivation the initial positive characteristic which represents the leading edge of the wave or disturbance will be denoted by C_{+1} and variables having the subscript 1 are values along C_{+1}.

The positive characteristics close to C_{+1} will be parameterized as follows:

> Choose some point on C_{+1} whose t coordinate is δt. Consider the negative characteristic emanating from this point. Let the point at which this negative characteristic intersects the boundary (or frontal motion) curve have the coordinates (x_o, t_o). Consider the positive characteristic, C_{+2} emanating from this point. Associate with this positive characteristic the parameter value δt.

Thus, the family of characteristics lying in the neighborhood of C_{+1} is parameterized by δt. Let C_{+2} denote either one particular member of the family or the entire family, depending on the context in which it is used. It should be noted that the functions u and c are known, a priori, along C_{+1}, but nowhere else in the region of motion, in particular along the class of curves C_{+2}.

Consider some negative characteristic between C_{+1} and C_{+2}. The non-dimensional equation of compatibility (34) with asterisks neglected demands (recalling the initial condition that $u_1 = 0$):

$$u - 2c + Gt = -2 c_1 + Gt \qquad (52)$$

It has been shown by equation (39), that:

$$c_1 = 1 - \frac{1}{2} G t_1 \tag{53}$$

Combining (52) and (53)

$$u - 2c = -2 + G(2 t_1 - t) \tag{54}$$

The equation of compatibility along C_{+2} from (34) requires:

$$u + 2c + Gt = u_o + 2 c_o + G t_o \tag{55}$$

where the subscript o indicates the first point on C_{+2}. For any point on C_{+2} (54) and (55) hold simultaneously. Addition and subtraction of these equations yield the following expressions for u and c at any point, x, t on C_{+2}:

$$u = \frac{u_o}{2} + c_o + G\left(\frac{t_o}{2} - t + t_1\right) - 1 \tag{56}$$

$$c = \frac{u_o}{4} + \frac{c_o}{2} + G\left(\frac{t_o}{4} \frac{-t_o}{2}\right) + \frac{1}{2} \tag{57}$$

Now from equation (33) the differential equation for C_{+2} is:

$$\frac{dx}{dt} = u + c$$

then from (56) and (57) the differential equation for C_{+2} becomes:

$$\frac{dx}{dt} = \frac{3 u_o}{4} + \frac{3 c_o}{2} + G\left(\frac{3 t_o}{4} + \frac{t_1}{2} - t\right) - 1/2 \tag{58}$$

Now let t differ from t_1, the "known" value on C_{+1}, by a small perturbation, ϵ. It follows that:

$$t_1 = t - \epsilon \quad , \tag{59}$$

where ϵ will be considered a function of t and δt.

and (59) may be rewritten:

$$\frac{dx}{dt} = \frac{3u_o}{4} + \frac{3c_o}{2} + G\left[\frac{3t_o}{4} - 1/2\,(t + \epsilon)\right] - 1/2$$

Integration of this equation from the first point on $C_{+2}(x_o, t_o)$ to any other point on $C_{+2}(x, t)$ yields

$$x = x_o + \frac{3}{4}(u_o + 2c_o + Gt_o - \frac{2}{3})\,(t - t_o) - G\,\frac{(t^2 - t_o^2)}{4} - \frac{G}{2}\int_{t_o}^{t} \epsilon\ dt \tag{60}$$

Now if the equation of compatibility for the negative characteristics (52) is applied to the negative characteristic that passes through (x_o, t_o) it follows that

$$u_o - 2c_o + Gt_o = -2c_1 + G\,\delta t \tag{61}$$

Applying equation (53) for $t_1 = \delta t$ and substituting in equation (61) yields the following expression for c_o:

$$c_o = 1/2\,[u_o + 2 + G(t_o - 2\,\delta t)] \tag{62}$$

Substitution of this expression into equation (60) yields the following equation for C_{+2}:

$$x = t - G\frac{t^2}{4} + x_o + \frac{3}{2}[u_o + G(t_o - \delta t)]\,(t - t_o) - t_o + \frac{Gt_o^2}{4} - \frac{G}{2}\int_{t_o}^{t} \epsilon\ dt \tag{63}$$

Given this equation for C_{+2}, the procedure for determining the initial point of breaking appears straightforward:

1. By eliminating x between equation (63) and the equation for C_{+1} (40), an expression for the time at which C_{+2} intersects C_{+1}, t_b, would be obtained. Clearly t_b would be a function of u_o, x_o, t_o, and ϵ. Since u_o, x_o, t_o, and ϵ are all functions of δt, t_b could be written as $t_b(\delta t)$.
2. Then, if $t_b(\delta t)$ were taken to the limit as δt approaches zero, the time of initial breaking, t_B, would be derived. Thus, a definition of the initial breaking time is

$$t_B = \lim_{\delta t \to o} t_b(\delta t)$$

where $t_b(\delta t)$ are the t-coordinates of the intersections of the C_{+2} family with C_{+1}.

The difficulty with this procedure is that u_o, x_o, t_o and ϵ are all unknown functions of δt. It will be shown that the functional relationships between δt and u_o, x_o, and t_o can be approximated. The main difficulty occurs for ϵ. Various approximations for the integral of ϵ were applied which apparently yielded good approximations for the computed values of the initial breaking time, but these all failed when taken to limiting values of the modeling parameters. An outline of the procedure for determining $t_b(\delta t)$ which was finally adopted follows:

1. Derive an approximate relationship between x and t for any given negative characteristic between C_{+1} and C_{+2}.

2. Eliminate x between the resulting approximation and the equation for C_{+2} (63). This yields $f(t, x_o, t_o, u_o, \delta t, \epsilon) = 0$ which turns out to be an integral equation in ϵ.
3. Solve this equation in the form $t = h(x_o, t_o, u_o, \delta t, \epsilon)$.
4. From the definition (59) of the perturbation quantity, ϵ,

$$\epsilon(t, \delta t) = t - t_1$$

where t is the t-coordinate on C_{+2} and t_1 is the corresponding t-coordinate on C_{+1}. Now, at the intersection of C_{+2} and C_{+1}, $t = t_1 = t_b(\delta t)$. Therefore,

$$\epsilon(t_b, \delta t) = 0$$

and an expression for t_b follows immediately from step 3, as

$$t_b = h(x_o, t_o, u_o, \delta t, 0)$$

5. Then, t_B is determined as discussed above.

The details involved in carrying out this procedure will be found below.

Consider the differential equation, (33), for any negative characteristic:

$$\frac{dx}{dt} = u - c$$

Now this differential equation cannot be integrated since the functions u and c between $C_{+2}(x,t)$ and $C_{+1}(x_1, t_1)$ are unknown. However, the finite difference approximation analogous to equation(42b) may be used here yielding

$$\frac{x - x_1}{t - t_1} = 1/2 \ [u - c - c_1] \tag{64}$$

Now if equations (56), (57) and (62) are substituted into (64) and use is made of the equation for C_{+1} (40), namely

$$x_1 = t_1 - G\frac{t_1^2}{4}$$

then the following is obtained:

$$x = t_1 - \frac{G}{4}t_1^2 + (t - t_1)\left[\frac{u_o}{4} + G\left(\frac{t_o - \delta t}{4} - \frac{t}{2} + t_1\right) - 1\right] \tag{65}$$

If the "perturbation definition" for the relationship between t and t_1, (59), is now applied to (65) the following approximate expression for a negative characteristic between C_{+1} and C_{+2} is obtained:

$$x = t - \frac{Gt^2}{4} + \epsilon\left[\frac{u_o}{4} - 2 + G\left(\frac{t_o - \delta t}{4} + t - \frac{5\epsilon}{4}\right)\right] \tag{66}$$

At any point (x, t) on C_{+2} equations (63) and (66) hold simultaneously. It follows that:

$$x_o + 3/2\left[u_o + G(t_o - \delta t)\right](t - t_o) - t_o + \frac{Gt_o^2}{4} - \frac{G}{2}\int_{t_o}^{t} \epsilon \, dt$$

$$- \epsilon\left[\frac{u_o}{4} - 2 + G\left(\frac{t_o - \delta t}{4} + t - \frac{5\epsilon}{4}\right)\right] = 0$$

Thus, an integral equation for ϵ has been derived. If this equation is differentiated with respect to time the following differential equation for ϵ is obtained:

$$\frac{d\epsilon}{dt} = \frac{6\,[u_o + G\,\epsilon_o - G\,\epsilon]}{u_o - 8 + G\,\epsilon_o + 4\,Gt - 10\,G\epsilon} \tag{67}$$

where $\epsilon_o \equiv t_o - \delta t$, the value of ϵ at the first point on C_{+2}. If ϵ and t are redefined as:

$$\epsilon = \frac{1}{G}\left[E + h\right]$$

and

$$t = \frac{1}{G}\left[T + k\right]$$

where h and k are constants, (67) may be rewritten:

$$\frac{dE}{dT} = \frac{6\,[u_o + G\,\epsilon_o - h] - 6\,E}{u_o - 8 + G\,\epsilon_o + 4\,k - 10\,h + 4\,T - 10\,\epsilon} \tag{68}$$

Now h and k may be defined so that all constant terms in the differential equation vanish, i.e.

$$h = u_o + G\,\epsilon_o$$

$$k = 2 + \frac{9}{4}\,(u_o + G\,\epsilon_o)$$

Then equation (68) can be rewritten

$$\frac{dT}{dE} + \frac{2}{3E}\,T = \frac{5}{3}$$

This is a first order linear differential equation which is readily solved by standard techniques. The solution follows:

$$T = B\,E^{-2/3} + E$$

where B is the constant of integration. Transforming this solution back into ϵ, t coordinates yields:

$$t = \frac{1}{G}\left\{2 + \frac{5}{4}(u_o + G\epsilon_o) + B\left[G\epsilon - (u_o + G\epsilon_o)\right]^{-2/3} + G\epsilon\right\} \qquad (69)$$

To evaluate B consider equation (69) at $t = t_o$ in which case $\epsilon = \epsilon_o$ by definition. Then

$$B = \left[G t_o - 2 - 5/4\ u_o - \frac{9}{4}\ G\epsilon_o\right] u_o^{\,2/3}$$

From the previous discussion about the relationship between the initial breaking of the wave and the convergence of the characteristics it is clear that when $\epsilon = 0$, $t = t_b$ the time at which C_{+2} intersects C_{+1}. Therefore, substitution of the expression for B into equation (69) and then letting $\epsilon = 0$ yields the following approximate relationship for t_b:

$$t_b = \frac{1}{G}\left\{2 + \frac{5}{4}(u_o + G\epsilon_o) + \left[G t_o - 2 - \frac{5}{4}u_o - \frac{9}{4}\ G\epsilon_o\right]\left[\frac{u_o}{u_o + G\epsilon_o}\right]^{2/3}\right\} \qquad (70)$$

From equation (36): $u_o = a \sin t_o$

It is now assumed that δt is taken small enough so that $\sin t_o \approx t_o$ and ϵ_o is replaced by its definition $(t_o - \delta t)$. Then, equation (70) becomes:

$$t_b = \frac{1}{4G}\left\{8 + 5\left[(a + G)\, t_o - G\,\delta t\right] - \left[8 - 5(a + G)\, t_o - 9\, G\,\delta t\right]\left[\frac{a\, t_o}{(a+G)\, t_o - G\,\delta t}\right]^{2/3}\right\} \qquad (71)$$

From the definition of the point (x_o, t_o), it is clear that t_o is a function of δt. An approximation to this relationship will now be derived.

Consider the finite difference form of the differential equation for the negative characteristic between the first point on $C_{+2}(x_o, t_o)$ and the second point on $C_{+1}(x_1, \delta t)$. This equation will be of the same form as equation (64):

$$x_o - x_1 = \frac{1}{2} (u_o - c_o - c_1) (t_o - \delta t) \tag{72}$$

From the equation of compatibility for this characteristic (see equation [43b]):

$$- c_o = \frac{1}{2} [-2 c_1 + G \delta t - u_o - G t_o] \tag{73}$$

Now from previously derived expressions c_1 (53) and x_1 (40) may be eliminated from equations (72) and (73). As has been pointed out u_o may be replaced by $a t_o$ for sufficiently small $t_o (\delta t)$. From equation (35)

$$x_o = a (1 - \cos t_o)$$

which becomes, after expansion of cos t_o in a Taylor's series,

$$x_o = a \frac{t_o^2}{2}$$

for sufficiently small $t_o (\delta t)$. Substituting these expressions for u_o and x_o into (72) and (73) and eliminating c_o between them yields, after simplification:

$$(G + a) t_o^2 + [4 - (3 G - a) \delta t] t_o + 3 G \delta t^2 - 8 \delta t = 0$$

Solving for t_o:

$$t_o = \frac{(3\,G - a)\,\delta t - 4 \pm \sqrt{[4 - (3\,G - a)\,\delta t]^2 - 4\,(G + a)\,(3\,G\,\delta t^2 - 8\,\delta t)}}{2\,(G + a)}$$

It is clear that the positive radical must be used since t_o must be zero when δt is zero. Now if the radical is simplified and expanded in a power series, neglecting terms involving powers in δt of three and higher, an approximation for t_o follows:

$$t_o \cong 2\,\delta t - \frac{(6a + G)}{4}\,\delta t^2$$

Substitution of this approximation in equation (71) yields, after simplification:

$$t_b = \frac{1}{4G}\left\{8 + (10\,a + 5\,G)\,\delta t - [8 + (10\,a + G)\,\delta t]\left[\frac{2\,a - 3/2\,a^2\,\delta t}{2\,a + G - 3/2\,a\,(a+G)\,\delta t}\right]^{2/3}\right\} \tag{74}$$

In this form of the approximation for t_b, terms involving higher order powers of δt have been neglected.

As previously discussed, the time of initial breaking follows from (74) by taking the limit as δt goes to zero. Thus,

$$t_B = \frac{2}{G}\left[1 - \left(\frac{2a}{2\,a + G}\right)^{2/3}\right] \tag{75}$$

From equation (40):

$$x_B = t_B - \frac{G}{4}\,t_B^2 \tag{76}$$

Thus, by equations (75) and (76) the point of initial breaking is determined. Equation (75) will now be examined for various limiting values of acceleration and slope.

Consider first the case of a zero underlying slope (G = 0). Under this condition the expression is undefined, but the limit as G goes to zero gives:

$$t_B = \frac{2}{3a} \tag{77}$$

Parenthetically note, that the differential equation for ϵ (67) when G = 0 becomes

$$\frac{d\epsilon}{dt} = \frac{6\, u_o}{u_o - 8}$$

Solving this equation for $t(\epsilon)$ and using the same procedure as for arbitrary G the following is obtained:

$$t_b = \left(\frac{8 - 2\, a\, \delta t}{12\, a - 9\, a^2\, \delta t}\right)\left(1 - \frac{3}{2}\, a\, \delta t\right) + 2\, \delta t$$

Then, setting $\delta t = 0$ as before

$$t_B = \frac{2}{3a}$$

which is the same result as equation (77).

Note that for G = 0, from equation (76), $x_B = t_B$. These relationships are non-dimensional. If they are made dimensional the following relations result for the zero slope case:

$$t_B = \frac{2}{3\alpha}\, c_o \tag{78}$$

$$x_B = \frac{2}{3\alpha} c_o^2 \tag{79}$$

where α is the dimensional initial acceleration given by equation (32) as:

$$\alpha = \frac{c_o^2 a}{x_o}$$

where a is non-dimensional.

Abdullah (1949) has performed a mathematical analysis of a model such as that used here with zero slope and with the "front" moving from rest with constant acceleration. He derived an analytical solution to the governing equations. From the analytical solution he derived values for the point of initial breaking which are exactly those given by (78) and (79).

Consider the case of an infinite slope ($G = \infty$). Under this condition $t_B = x_B = 0$. This trivial result is to be expected.

Thus, the derived solution for the position and time of initial breaking is verified in so far as it gives correct results for the various extremes in the modeling parameters. As a further verification consider the results computed from the perturbation solution for the various values of initial acceleration and slope used in the finite difference approximation computations. These results are presented in Table II. For comparison purposes, the results from the numerical integration approximation and the perturbation solution, are presented in Figures 7 and 8.

An examination of the derivation of the perturbation solution reveals that it is applicable to <u>any</u> model in which:

Table II: Perturbation Solution Results

	$a^* = 0.5$		$a^* = 1.0$		$a^* = 2.0$	
η_x	x_B^*	t_B^*	x_B^*	t_B^*	x_B^*	t_B^*
0	1.33	1.33	0.67	0.67	0.333	0.333
.01	1.26	1.28				
.02	1.19	1.23	0.63	0.64	0.323	0.326
.03	1.13	1.19				
.04	1.08	1.15	0.60	0.62	0.315	0.320
.05	1.03	1.11				
.06	0.98	1.07	0.57	0.59	0.308	0.315
.07	0.94	1.04				
.08	0.90	1.01	0.54	0.57	0.299	0.309
.09	0.87	0.98				
.10	0.84	0.95	0.51	0.55	0.291	0.302
.11	0.81	0.92				
.12	0.78	0.90	0.49	0.53	0.284	0.297
.13	0.75	0.87				
.14	0.72	0.85	0.47	0.52	0.277	0.292
.15	0.70	0.83				
.16	0.68	0.81	0.45	0.50	0.271	0.287
.17	0.66	0.79				
.18	0.64	0.77	0.43	0.49	0.263	0.282
.19	0.62	0.76				
.20	0.60	0.74	0.42	0.47	0.257	0.276

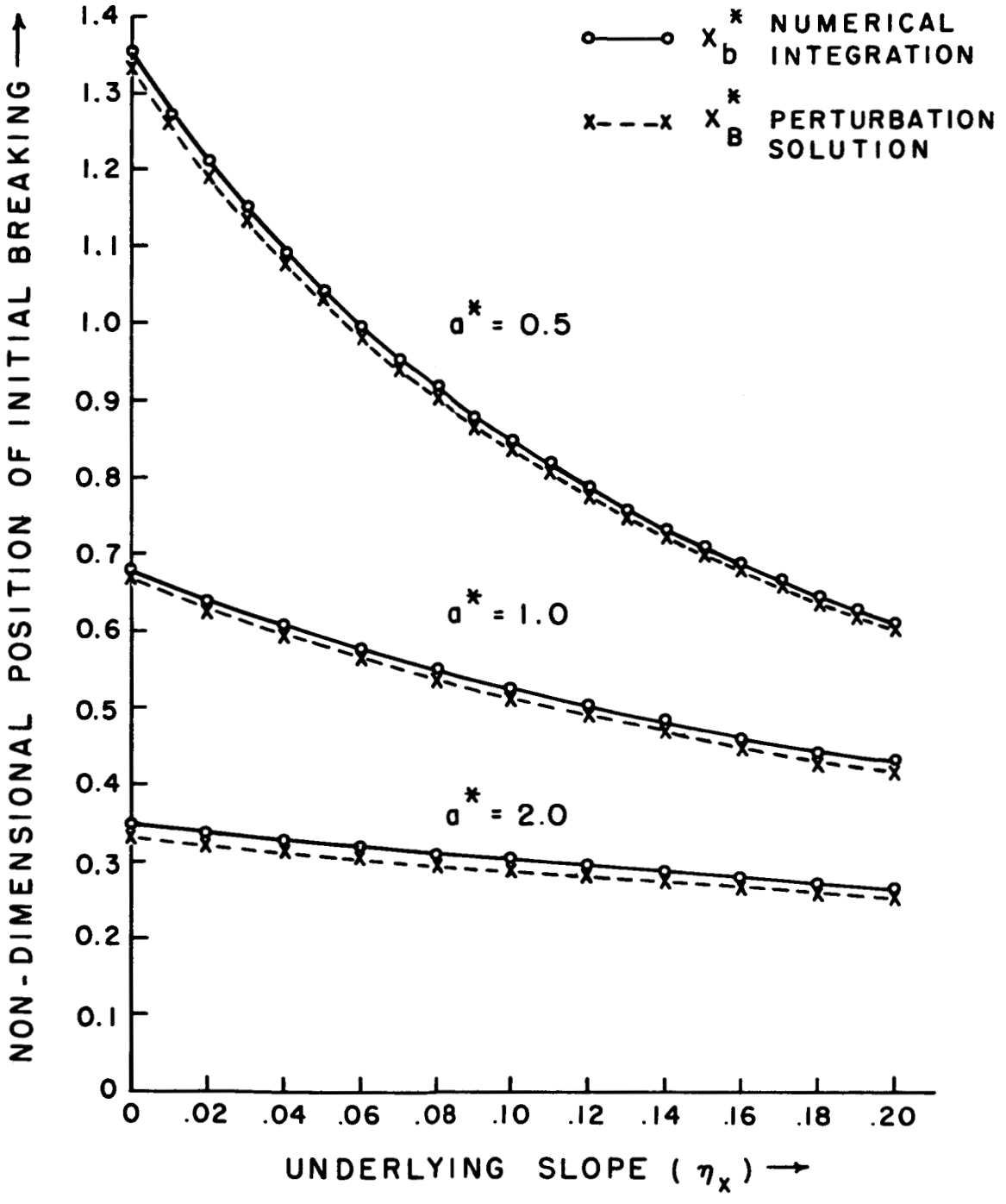

Figure 7. Comparison of numerically integrated and perturbation solution results for initial breaking position

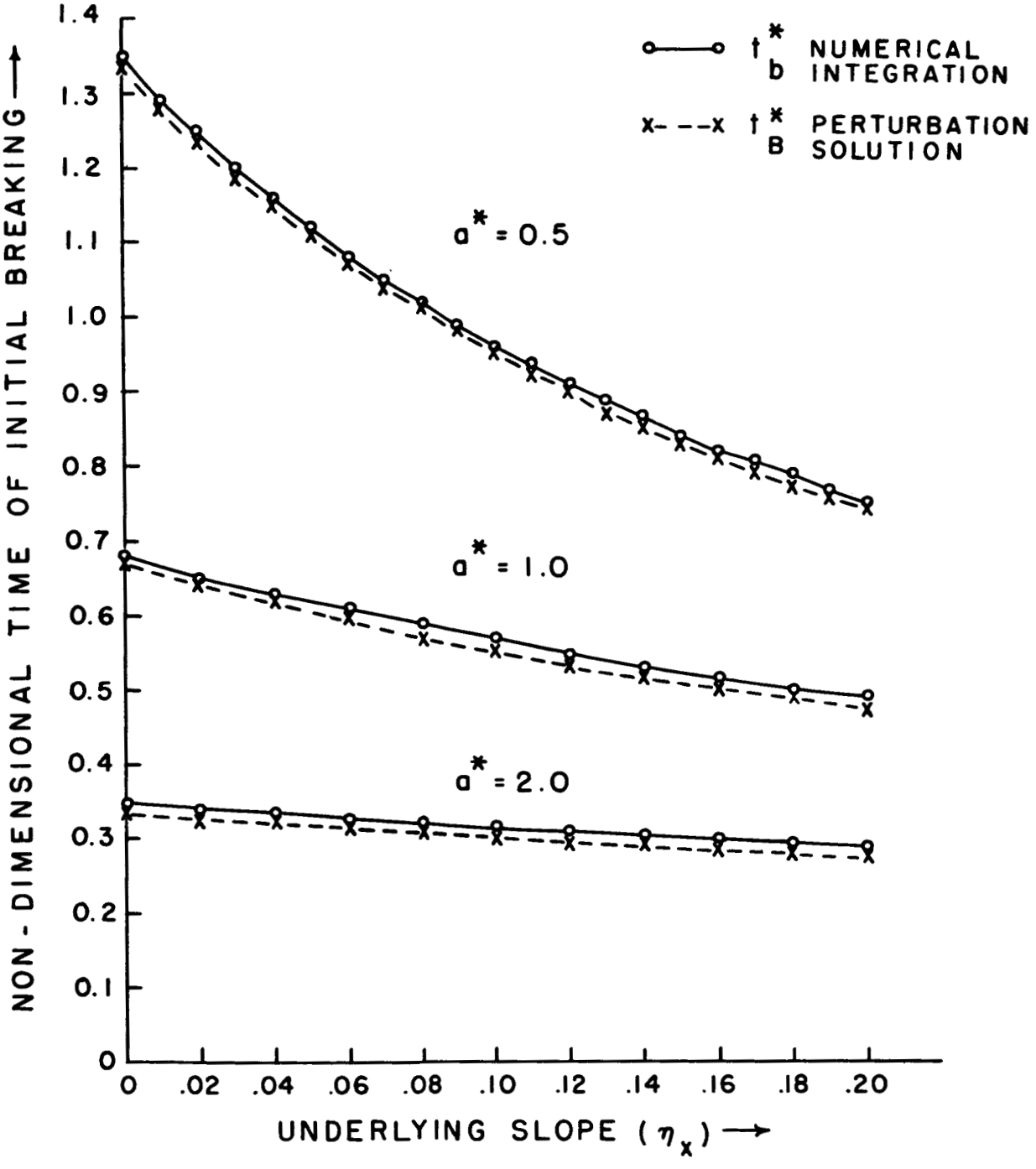

Figure 8. Comparison of numerically integrated and perturbation solution results for time of initial breaking time.

1. the equation of motion is sufficiently regular, i.e., has at least three continuous derivatives,
2. the wave generating mechanism starts from rest with a non-dimensional acceleration, $\underline{a}$,
3. all other aspects of the model are the same as the model used in this study.

This generalization of the perturbation result follows from the approximations made for the functions $x_o(t_o)$ and $u_o(t_o)$.

The case treated by Abdullah (1949), which was previously discussed, satisfies the three above conditions with the special property that $\underline{a}$ remains constant. It is, therefore, not surprising that his result for the initial breaking point agrees with the result derived here.

If the equations for the time (75) and position (76) of initial breaking are made dimensional the following are obtained:

$$t_B = \frac{2}{s}\sqrt{\frac{h_o}{g'}}\left[1 - \left(\frac{1}{1+\frac{g's}{2\alpha}}\right)^{2/3}\right] \tag{80}$$

$$x_B = \sqrt{g'h_o}\ t_B - \frac{sg'}{4}\ t_B^2 \tag{81}$$

Formulas (80) and (81) determine the point of initial breaking in terms of:

s - the underlying slope

h_o - the undisturbed height of the interface (inversion)

g' - the density weighted gravitational acceleration

α - the initial "frontal" acceleration

for any model satisfying the three conditions specified above.

It follows that the effect of the underlying slope on the point of initial breaking, under the idealized conditions of the model, is explicitly given by (80) and (81).

7. Conclusion

As mentioned in Section 1 of this report, Tepper and Abdullah have advanced the hypothesis that the atmospheric breaking wave (or pressure jump) is a cause of pre-cold frontal squall lines. If this hypothesis is true it might be reasonable to expect that the distance between the modelled point of initial breaking and the "front" should be of the same order of magnitude as the distance which is observed in the atmosphere between the front and the squall line. The latter distance is readily obtainable from standard meteorological charts. Therefore, an attempt will be made to investigate the consistency of the perturbation solution with the physical hypothesis by means of observations under the assumption of a very simple model.

In an analysis of twenty-four pre-cold frontal squall lines, Miller (1958) found that the composite squall line was about 180 nautical miles ahead of the composite cold front. The mean geographical position of the squall line centers was in southern Illinois. In this region the underlying slope, when averaged over distances of the order of a hundred nautical miles,is effectively zero.

Consider, first, the results of the numerical computations. From Table I, for a zero slope, the maximum x_b is 13.5 km. From the equation of frontal motion (30), the position of the front at $t = t_b =$ 770 seconds can be determined. The distance between the squall line and the front is approximately 9.6 km or about 5.2 nautical miles. This is almost one and a half orders of magnitude less than the distance reported by Miller. The wave begins to break close to the front

because of the high initial acceleration (112 kts/hr) used in the model. While instantaneous frontal accelerations as high as this may be observed, on the average frontal accelerations must be considerably smaller.

Of course, without the perturbation solution, the point of initial breaking cannot be predicted in advance of the computations. Also, for the sake of speed in computing the results a high initial acceleration is not unreasonable. Thus, without the perturbation solution, in order to obtain results which would be comparable to those obtained by Miller, many experiments would have to be carried out on the computer. Such an expensive trial and error process would not yield any conclusive results. However, with the perturbation solution and a sufficiently simple equation for the motion of the "front", it is a straightforward procedure to determine the initial frontal acceleration necessary to achieve various distances between the front and the initial point of breaking.

Consider the simplest model which permits use of the perturbation solution, i.e., a model with the "front" starting from rest with a constant acceleration, α. In this case the equation for the frontal position, x_F, at the time of initial breaking, t_B, is:

$$x_F = \frac{1}{2}\alpha\ t_B^2$$

From this formula and (78) and (79) it can be shown that the acceleration, α (kts/hr), which is necessary to cause the wave to begin breaking at a distance, d (nautical miles), from the front is given by:

$$\alpha = 544.44/d$$

where c_o has been taken as 35 kts in (78) and (79). This is approximately the value of c_o which was used in all of the previous computations. The required accelerations and resulting times of intial breaking corresponding to various values of $\underline{d}$ are given in Table III.

Table III: Computations for a Simple Atmospheric Model

Distance between front and initial point of breaking d(n.m.)	Constant frontal acceleration α (kts/hr)	Time of initial breaking t_B (hr)
100	5.4	4.3
125	4.4	5.3
150	3.6	6.5
175	3.1	7.5

Thus, to obtain values of $\underline{d}$ for this simple model which are of the same order of magnitude as Miller's results, frontal accelerations are required which are certainly observable in the atmosphere. The time of initial breaking is merely presented to indicate the time scales required for the development of the phenomena which may be associated with the breaking atmospheric wave.

It would be ideal if observations of frontal accelerations were available in cases of squall line formation. Unfortunately, standard meteorological observations will permit only computations of approximate frontal accelerations averaged over six hours. Thus, one must evaluate the reasonableness of accelerations of the order of those presented in Table III. It is hoped that other measures of the plausibility of both the Tepper-Abdullah hypothesis will be evaluated in the near future.

These measures will be, in all likelihood, of an indirect nature just as the very simple one presented above.

Acknowledgements

The author wishes to express his appreciation to Dr. Nathan Newman for the many hours he spent patiently discussing the mathematical analysis and the presentation of the work reported herein; to Dr. Herman Newstein for many helpful suggestions concerning the numerical integration of the characteristic equations; to Captain Arthur Ward for his invaluable assistance during the programming and computing phases of the work; to Professor James E. Miller for performing the unenviable task of correcting the manuscript; to Mrs. Gertrude Fisher who turned out clear diagrams from confused sketches; and to Mrs. Lillian Bloom and Mrs. Elsie Miller who converted an illegible manuscript into a finished report.

References

Abdullah, A.J., 1949: Ccyclogenesis by a purely mechanical process. J. Meteor., V.6, No.2, pp.86-97.

_____, 1955: The atmosphere solitary wave. Bull. Amer. Meteor. Soc., V.36, No.10, pp.511-518.

_____, 1961: Seminar at New York University.

Bronwell, A., 1953: Advanced Mathematics in Physics and Engineering. Mc-Graw-Hill Book Company, Inc., New York, pp.110-111.

Courant, R. and K.O. Friedrichs, 1948: Supersonic Flow and Shock Waves. Interscience, New York.

Lamb, H., 1945: Hydrodynamics, 6th edition. Cambridge University Press and New York Dover Publications, p.423.

Miller, J.E., 1958: Composite charts of some synoptic features of squall lines. Severe Weather Phenomena, Final Report, Contract No. AF 19(604)-1387, Dept. of Meteor. and Ocean., New York University, pp.33-47.

Miller, J.E. and R.S. Greenfield, 1962: Status report of breakers project. Contract No. NsG-168-61, Project No.885, Dept. of Meteorology and Oceanography, New York University, 6 pp.

Sauer, R., 1952: Anfangswertprobleme bei partiellen Differential gleichungen, Springer-Verlag, Berlin, 229 pp.

Stoker, J.J., 1948: The formation of breakers and bores. Communications on Applied Mathematics, V.1, No.1, pp.1-87.

Tepper, M., 1950: A proposed mechanism of squall lines: the pressure jump line. J. Meteor., V.7, No.1, pp.21-29.

Appendix

The FORTRAN program which was used to determine the point of intersection of C_{+1} and C_{+2} is presented below. The following definitions relate the notation used in the program to that used in the text:

A1 = a
DT = δt
S = η_x
GR = g
W = $1/x_o$
CO = c_o
HO = h_o
T = t
X = x
C = c
U = u
DD = $(\rho - \rho_o)/\rho$

All variables and constants are non-dimensional with the exception of GR(g), HO(h_o), CO(c_o) and W(x_o^{-1}) which are all in c.g.s. units. The numbers associated with X, T, U, and C are the same as the subscripts attached to x, t, u, and c in the text. All other letters are for variables and constants used in the course of the computations. The program follows:

```
      READ 9000, A1
      READ 9000, DT
1     READ 9000, S, DD, HO
      GR = 980.616
      W = 0.000001
      CO = SQRT (GR*DD*HO*100000.0)
```

```
      G=S/ (0.1*HO)
      T3 = DT
      X3 = T3* (1.0-0.25*G*T3)
      C3 = 1.0-0.5*G*T3
      E = 0.02
      E2 = 0.002
      E3 = 0.0002
      K = 1
      T4 = T3
      A = -4.0*C 3+ G*T3
      B = 4.0*A1 -4.0*X3 + A*T3
18    DT 1 = 0.5*E
      NIT = 1
      FF = 0
25    D = (G*T4 - A - G*T3) *T4+ B
      R = 0.5* (T4 - T3)*SIN(T4)+ 2.0* COS(T4)
      F = D - 2.0*A1*R
      IF (F) 29, 39, 30
29    IF  (F+E) 31, 38, 38
30    IF  (F-E)  38, 38, 31
31    IF (F*FF) 32, 34, 34
34    IF (NIT - 1000) 35, 35, 42
35    NIT = NIT + 1
      T4 = T4+ DT1
      FF = F
      GO to 25
32    IF   (2-K)  37, 38, 38
37    T4 = T4 - 0.00005
      GO  TO  39
38    IF   (2-K)   39, 33, 36
36    E = E2
      GO  to  24
33    E = E3
24    T4 = T4 - DT1
      K = K+ 1
      GO  TO  18
39    X4 = A1* (1.0 - COS(T4))
      U4 = A1*SIN(T4)
      C4 = 0.5* (U4+ 2.0*C3 - G* (T3 - T4))
      Z = U4+ 2.0*C4+ G* T4
      IF (SENSE SWITCH  1) 40, 43
40    PUNCH 9006
      PUNCH  9000, X3, T3, C3
      PUNCH  9000, X4, T4, C4, U4
      GO  TO  43
42    PRINT  9001, T1
      GO  TO  950
```

```
   43  T1=T3
       X1=X3
       C1=C3
       T2=T4
       X2=X4
       C2=C4
       U2=U4
   T3= T3=T1+DT
       X3=T3*(1.0-0.25*G*T3)
       C3=1.0-0.5*G*T3
       A=U2+C2
       B=-C3
       C4=0.25*(Z-2.0*B-G*T3)
       D=0.5*(Z+2.0*B+G*T3)
       Q1=2.0*(X3-X2)-D*(T3-T2)
       Q3=2.0*C4+A-B-G*(T3-T2)
       T4=(Q1+Q2)/Q3
       U4=D-G*T4
       X4=X2+0.5*(U4+C4+A)*(T4-T2)
       IF(SENSE SWITCH 1)66,67
   66  PUNCH 9000, X3, T3, C3
       PUNCH 9000, X4, T4, C4, U4
   67  IF(T3-T4)43, 68, 71
   68  XX=X4
       TT=T4
       GO TO 75
   71  B-C1
       TT=(X1-X2+A*T2-B*T1)/(A-B)
       XX=X2+A*(TT-T2)
   75  TT1=TT/(W*CO)
   78  IF(SENSE SWITCH 3)80, 90
   80  PRINT 9000, XX, TT
   90  PUNCH 9002
       PUNCH 9003, S, DD, HO, CO
       PUNCH 9004
       PUNCH 9005, XX, TT, XX1, TT1
       PUNCH 9009
       GO TO 1
 9000  FORMAT (F10.5, F10.5, F10.5, F10.5)
 9001  FORMAT(28H FAILED TO CONVERGE T(I, J)=F10.5)
 9002  FORMAT(34H SLOPE  DELTADEN        HO        CO)
 9003  FORMAT (F7.3, F12.5, F6.1, F14.5)
 9004  FORMAT(42H       XX          TT          XX1         TT1)
 9005  FORMAT (F10.5, F10.5, F12.5, F12.5)
 9006  FORMAT(36H)      X           T           C       U)
 9009  FORMAT(1H )
  950  STOP
       END
```